DOI: 10.1002/chem.201000773

Isomeric Squaraine-Based [2]Pseudorotaxanes and [2]Rotaxanes: Synthesis, Optical Properties, and Their Tubular Structures in the Solid State

Min Xue,[a, b] Yong-Sheng Su,[a, b] and Chuan-Feng Chen*[a]

Abstract: On the basis of formation of [2]pseudorotaxane complexes between triptycene-derived tetralactam macrocycles **1a** and **1b** and squaraine dyes, construction of squaraine-based [2]rotaxanes through clipping reactions were studied in detail. As a result, when two symmetrical squaraines **2d** and **2e** were utilized as templates, two pairs of isomeric [2]rotaxanes **3a–b** and **4a–b** as diastereomers were obtained, owing to the two possible linking modes of triptycene derivatives. It was also found, interestingly, that when a nonsymmetrical dye **2g** was involved, there existed simultaneously three isomers of [2]rotaxanes in one reaction due to the different directions of the guest threading. The ^{1}H NMR and 2D NOESY NMR spectra were used to distinguish the isomers, and the yield of [2]rotaxane **5a** with the benzyl group in the wider rim of the host **1a** was found to be higher than that of another isomer **5b** with an opposite direction of the guest, which indicated the partial selection of the threading direction. The X-ray structures of **3b** and **4a** showed that, except for the standard hydrogen bonds between the amide protons of the hosts and the carbonyl oxygen atoms of the guests, multiple π···π stacking and C–H···π interactions between triptycene subunits and aromatic rings of the guests also participated in the complexation. Crystallographic studies also revealed that the [2]rotaxane molecules **3b** and **4a** further self-assembled into tubular structures in the solid state with the squaraine dyes inside the channels. In the case of **4a**, all the nonsymmetrical macrocyclic molecules pointed in one direction, which suggests the formation of oriented tubular structures. Moreover, it was also found that the squaraines encapsulated in the triptycene-derived macrocycles were protected from chemical attack, and subsequently have potential applications in imaging probes and other biomedical areas.

Keywords: rotaxanes · self-assembly · squaraines · triptycenes · tubular structures

Introduction

Pseudorotaxanes and rotaxanes, important classes of interlocked chemical species, have attracted increasing attention due to their specific structural features and wide applications in molecular machines and devices.[1,2] A [2]pseudorotaxane can be described as a molecular system in which a macrocycle (wheel) is threaded by a linear subunit (axle). The insertion of two bulky stoppers at the ends of the axle yields a [2]rotaxane. When the three-dimensional and nonsymmetrical macrocycle is used as the wheel, an axle with different terminal groups can insert into the macrocycle from both rims, thus leading to two isomeric [2]pseudorotaxanes or [2]rotaxanes. Early examples of isomeric [2]rotaxanes were reported by Kaifer et al. with an α-cyclodextrin as a wheel.[3] Later, Tian et al. reported the α-cyclodextrin-based unidirectional [2]rotaxanes controlled by the dethreading rate of the former [2]pseudorotaxnes.[4] Meanwhile, the calix[6]arene platform, as a new type of nonsymmetrical wheel, was reported by Arduini et al. and a series of unidirectional calix[6]arene-based [2]pseudorotaxanes or [2]rotaxanes were constructed with hydrogen-bonding interactions as the control elements.[5] The above examples have succeeded in the formation of oriented [2]rotaxanes, which have potential utility in the construction of unidirectional molecular devices with new properties. However, nonsymmetrical macrocycles that can be used in this context only focused on the α-cyclodextrins and calix[6]arene derivatives.

[a] M. Xue, Y.-S. Su, Prof. C.-F. Chen
Beijing National Laboratory for Molecular Sciences
CAS Key Laboratory of Molecular Recognition and Function
Institute of Chemistry, Chinese Academy of Sciences
Beijing 100190 (China)
Fax: (+86) 10-62554449
E-mail: cchen@iccas.ac.cn

[b] M. Xue, Y.-S. Su
Graduate School, Chinese Academy of Sciences
Beijing 100049 (China)

Supporting information for this article is available on the WWW under http://dx.doi.org/10.1002/chem.201000773.

Until now, less effort has been directed to develop the synthesis of alternative nonsymmetrical macrocycles. Such molecules present the opportunity for new unidirectional functional [2]rotaxanes. Isomeric phenomena on [2]rotaxanes investigated previously were caused by the direction of guest insertion. When the guest is symmetrical, can isomeric [2]rotaxanes still be formed by the effect of the host? This is also an interesting question to explore.

Squaraines are a family of fluorescent near-IR dyes with specific photophysical properties for wide potential applications in imaging, nonlinear optics, photovoltaics, and ion sensing.[6] However, they are susceptible to chemical attack and aggregation in polar solvents, which limit their applications.[7] Recent development of squaraine-based rotaxanes by Smith et al. provides efficient routes to solve both of these problems.[8] And some of the squaraine rotaxanes can act as fluorescent imaging probes and chemosensors.[9] Other examples of squaraine-based complexes came from the Na^+-complexed molecular cages.[10] The rotaxane-encapsulation is a new aspect for squaraine dyes and still has many undiscovered aspects, such as their novel structural features, interaction modes, and a "secondary" self-assembly.

Recently, we have been interested in developing new supramolecular systems based on triptycene with a unique 3D rigid structure.[11] As a result, we have synthesized one pair of novel triptycene-based tetralactam macrocycles **1a** and **1b** and found that they formed remarkably stable [2]pseudorotaxanes with the squaraine **2b**, which could subsequently protect the dye from polar solvents.[12] In this paper, we describe in detail the complexation of the macrocycles **1a** and **1b** with different functionalized squaraine derivatives. Consequently, we have designed and synthesized a series of squaraine-based [2]pseudorotaxanes and [2]rotaxanes. In particular, isomeric [2]pseudorotaxanes and [2]rotaxanes have been obtained from both the linking modes of triptycene derivatives and the directions of the guest insertion. Moreover, we also investigated the structures and photochemical properties of the interlocked molecules and interestingly found that the [2]rotaxanes further self-assembled into tubular structures in the solid state.

Results and Discussion

Design of isomeric squaraine-based [2]pseudorotaxanes and [2]rotaxanes: Our preliminary studies showed that the macrocycles **1a** and **1b** could encircle the squaraine dye **2b** to form two [2]pseudorotaxane complexes with association constants of $(6.8\pm0.3)\times10^5$ and $(1.3\pm0.3)\times10^6\,M^{-1}$ in chloroform, respectively.[12] With rigid 3D structures, triptycene derivatives can often form macrocycles with a pair of diastereomers due to different linking modes during the reaction process.[13] It is of interest to construct squaraine-based isomeric [2]pseudorotaxanes and [2]rotaxanes by using this new route (Scheme 1) and compare their structures and photochemical properties. To achieve this goal, symmetrical squaraines **2a–e** with different terminal groups were designed. We supposed to choose one squaraine with bulky stopper groups, which could prevent the unthreading of the squaraine through the triptycene-derived macrocycles and thus be used as a template to synthesize isomeric [2]rotaxanes by a clipping reaction.

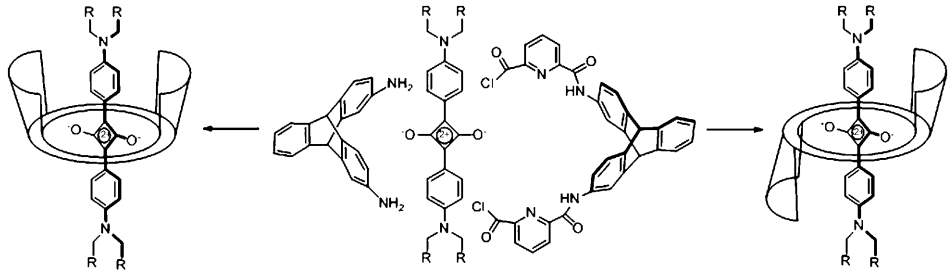

Scheme 1. Schematic representation of the two possible [2]pseudorotaxane or [2]rotaxane isomers due to different linking modes of the triptycene derivatives.

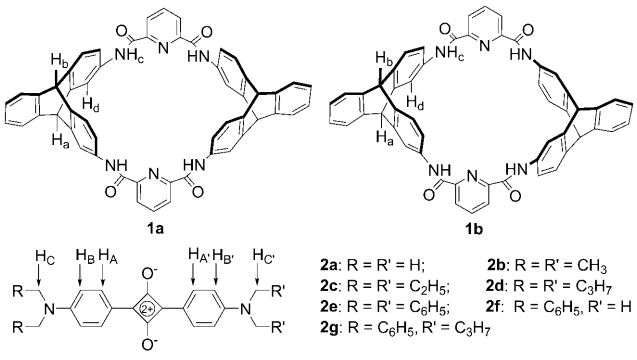

It was also known that macrocycle **1a** with a boat conformation displayed a nonsymmetrical environment for the squaraine molecule. We supposed if nonsymmetrical squaraine dyes were chosen as templates, isomeric [2]rotaxanes could be obtained from different directions of insertion of the squaraine guest (Scheme 2). For this purpose, the new nonsymmetrical squaraines **2f** and **2g** were designed.

Synthesis and structures of the [2]pseudorotaxanes and [2]rotaxanes: All the symmetrical squaraine derivatives **2a–e** were prepared by reacting two equivalents of the aniline precursors with squaraine acid by using a straightforward method.[14] Whereas nonsymmetrical squaraine derivatives

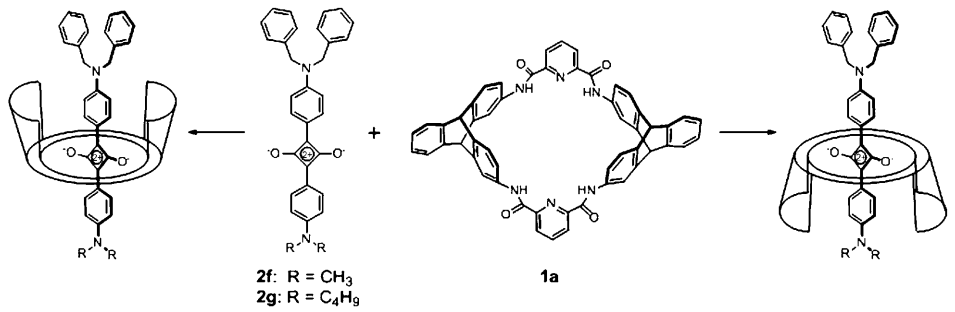

Scheme 2. Schematic representation of the two possible [2]pseudorotaxane or [2]rotaxane isomers due to different directions of squaraine insertion.

2f and **2g** were synthesized in two steps by the stable semi-squaraine intermediates by using standard literature procedures.[15]

From the formation of two [2]pseudorotaxane complexes **1a·2b** and **1b·2b**, it is easy to conclude that squaraine **2a** with smaller terminal groups than those of **2b** can also thread the wheels **1a** and **1b** to yield [2]pseudorotaxane complexes **1a·2a** and **1b·2a**. In the case of **2c**, as shown in Figure S17 in the Supporting Information, the ^{1}H NMR spectrum of host **1b** and guest **2c** (1:1) mixed in $CDCl_3$ displayed only one set of well-defined resonances differing greatly from those for the free host and guest, which indicated that squaraine **2c** could also penetrate through the macrocycle **1b** to form a [2]pseudorotaxane-type complex **1b·2c**. However, the ^{1}H NMR spectrum of a mixture of the host **1a** and guest **2c** (1:1) in $CDCl_3$ only exhibited signals for free **1a** and **2c**,[16] which suggested no insertion process at room temperature. When we tried to heat the mixture of **1a** and **2c** in $CDCl_3$ at 333 K for more than one day, the ^{1}H NMR spectra showed that with the signals for free **1a** and **2c** being weak, new signals appeared and gradually increased with time, which became predominant after six days (Figure 1). These observations suggested that [2]rotaxane **1a·2c** was obtained through slippage. When squaraines **2d** and **2e** were mixed with host **1a** or **1b** (1:1) in $CDCl_3$, the ^{1}H NMR spectra did not exhibit any signals for complexes, even after being heated at 333 K for several days. This indicated that the *N*,*N*-bis(*n*-butyl) and *N*,*N*-bis(benzyl) stopper groups are large enough to prevent the squaraines from forming [2]rotaxanes with triptycene-derived macrocycles **1a** and **1b** through the slippage method. For the nonsymmetrical squaraine **2f**, ^{1}H NMR spectroscopic studies showed the formation of complex **1b·2f**. The ^{1}H NMR spectrum of host **1a** and guest **2f** (1:1) mixed in $CDCl_3$ displayed two new sets of resonances, and the intensity of one set was higher than the other, which suggested that two isomeric [2]pseudorotaxane complexes based on **1a** and **2f** were obtained, and the complexation showed a slight selectivity. Similar to the cases of squaraines **2d** and **2e**, it was found that squaraine **2g** with two different bulky stoppers could not form [2]pseudorotaxane complexes with hosts **1a** and **1b** at room temperature or at 333 K (Scheme 3).

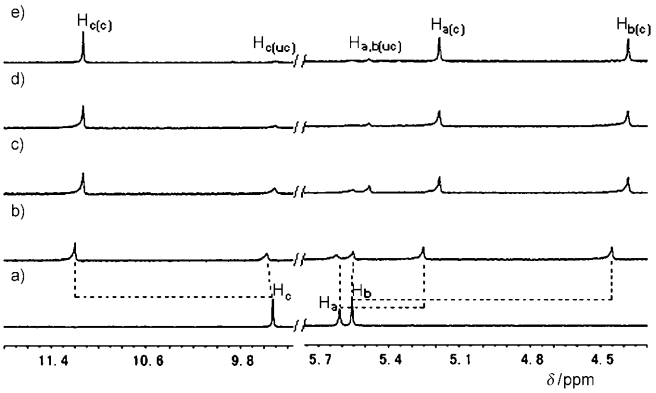

Figure 1. Time-dependent ^{1}H NMR spectra of **1a·2c** in $CDCl_3$ at 298 K (a), at 333 K after 1 d (b), at 333 K after 2 d (c), at 333 K after 4 d (d), at 333 K after 6 d (e). [**1a**]=[**2c**]=3.0 mM. Associated protons are labelled in structures **2a**–**f**.

According to the above results, squaraines **2d**, **2e**, and **2g** with bulky stopper groups were chosen as the templates to synthesize [2]rotaxanes through clipping reactions. Thus, squaraine-based [2]rotaxanes **3**–**5** were subsequently obtained by condensing pyridine-2,6-dicarbonyl dichloride and 2,7-diaminotriptycene in the presence of an appropriate squaraine derivative in total yields of 31–37% after purification by silica-gel column chromatography (Scheme 4).[17] When **2d** was used as the template, two different products **3a** and **3b** formed and showed the same peak at *m*/*z*: 1318.9 for M^+ and similar polarity, which suggested that they were a pair of diastereomers. Meanwhile, compounds **4a** and **4b** could also be obtained as isomers similar to the case of **3a** and **3b**. However, when the nonsymmetrical squaraine **2g** was used as a template, there existed three products with the same peak at *m*/*z*: 1386.8 for M^+ and with similar polarity, which meant three isomers were yielded during the formation of [2]rotaxanes **5**.

Structures of these isomeric [2]rotaxanes were first confirmed by ^{1}H NMR spectroscopy. As shown in Table 1 and associated atom labelling in the structures of **2a**–**f**, the

Table 1. Changes in chemical shift ($\Delta\delta$ [ppm]) for [2]rotaxanes **3**–**5**.

	a	b	c	A	B	C	A′	B′	C′
3a	−0.50	−0.70	1.77	0.88	0.69	0.28	−1.04	−0.63	−0.24
3b	−0.41	−0.46	1.95	−0.83	−0.37	−0.02			
4a	−0.35	−1.11	1.54	0.80	0.55	0.28	−1.04	−0.68	−0.26
4b	−0.29	−0.37	1.76	−0.92	−0.43	0.14			
5a	−0.36	−1.11	1.58	−1.08	−0.66	−0.26	0.90	0.63	0.27
5b	−1.14	−0.29	1.63	0.84	0.61	0.29	−0.9	−0.65	−0.25
5c	−0.68, −0.64	−0.21	1.92, 1.93	−0.97	−0.50	−0.02	−0.81	−0.52	−0.05

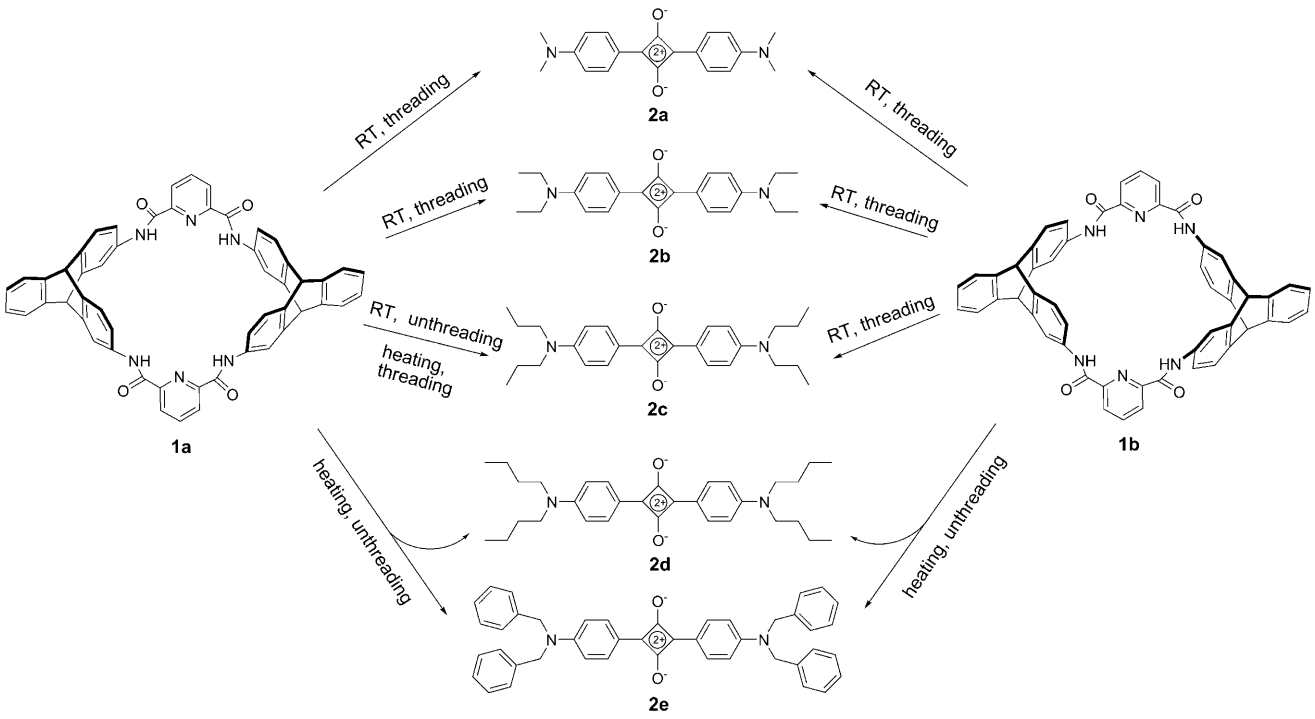

Scheme 3. Interaction modes between macrocycles **1a**–**b** and squaraines **2a**–**e**.

^{1}H NMR spectra of **3**–**5** all showed striking downfield shifts ($\Delta\delta = 1.54$–1.95 ppm) for H_c and upfield shifts ($\Delta\delta = -0.21$–-1.14 ppm) for H_a and H_b, which were well consistent with those of the [2]pseudorotaxanes, and thus indicated the formation of the [2]rotaxane-type complexes. For [2]rotaxanes **3** and **4**, protons $H_{A(A')}$, $H_{B(B')}$, and $H_{C(C')}$ in **3a** and **4a** displayed two sets of signals with one set upfield-shifted and the other downfield-shifted, which possibly resulted from the nonsymmetrical environment provided by the macrocycle. Protons $H_{A(A')}$, $H_{B(B')}$, and $H_{C(C')}$ in compounds **3b** and **4b** displayed only one set of signals that shifted upfield, which suggested a symmetrical environment. Compared to the *cis* macrocycle **1a** with the *trans* isomer **1b**, it was found that **1a** was a three-dimensional nonsymmetrical macrocycle with a boat conformation, which might induce the nonsymmetrical environment for the squaraines.[18] Thus, [2]ro-

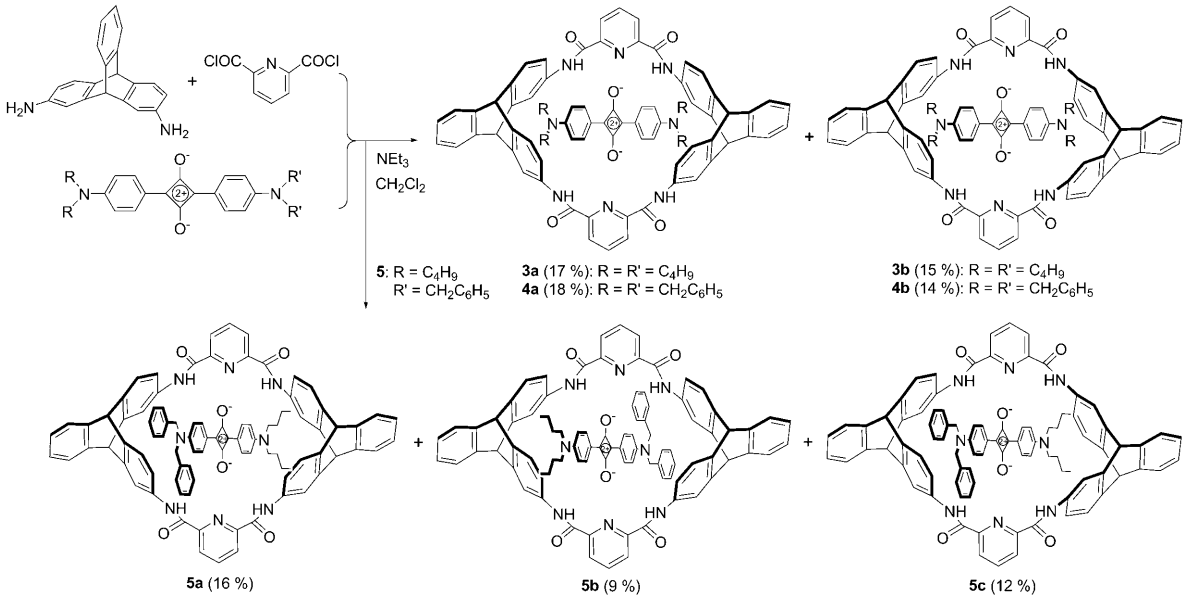

Scheme 4. Synthetic routes for [2]rotaxanes **3**–**5**.

taxanes **3a** and **4a** were confirmed as the *cis* isomers, whereas [2]rotaxanes **3b** and **4b** were the *trans* isomers. In the case of [2]rotaxanes **5**, the ^{1}H NMR spectra of the three isomers all became complicated because of the nonsymmetrical squaraine **2g**. It was found that both signals of H_{A-C} and $H_{A'-C'}$ in [2]rotaxane **5c** shifted upfield, whereas in [2]rotaxanes **5a** and **5b**, the signals of H_{A-C} displayed opposite shifts relative to those of $H_{A'-C'}$, which suggested that **5c** was the *trans* isomer and both **5a** and **5b** were *cis* isomers. The different shielding or deshielding effect on H_{A-C} and $H_{A'-C'}$ between **5a** and **5b** indicated the different directions of squaraine **2g**. 2D NOESY NMR spectroscopic studies provided the most diagnostic evidence for estimating the direction. An NOE signal of **5b** corresponding to the contacts between H_C of **2g** and H_d of **1a** was detected, which suggested the position of the narrower rim for the benzyl stopper group in **5b**.[19] In contrast, **5a** is the isomer with the benzyl group in the wider rim of host **1a** and the *n*butyl group in the narrower rim. From the synthetic conclusion it was known that the yield of **5a** (16%) was higher than that of **5b** (9%). This meant that the benzyl stopper group, which is larger and more rigid than the *n*butyl stopper group, preferentially located in the wider rim of macrocycle **1a**. Thus, partially oriented squaraine-based [2]rotaxanes were formed. Besides the two *cis* isomers **5a** and **5b**, the *trans* isomer **5c** also had a distinct characteristic different from other *trans* isomers **3b** and **4b**, which was the partition of two sets of signals for bridging CH proton H_a and NH proton H_c due to the nonsymmetrical environment induced by squaraine **2g** with different stopper groups.

The X-ray crystal structures of [2]rotaxanes **3b** and **4a** are illustrated in Figure 2.[20] In both cases, the hydrogen-bonding interactions ($d_{H\cdots O}=2.22$ Å, $\theta_{N-H\cdots O}=144.07°$ for **3b**, and $d_{H\cdots O}=2.19$ Å, $\theta_{N-H\cdots O}=150.34°$ for **4a**) between the amide protons of hosts and the carbonyl oxygen atoms of guests exist and they are a little stronger than the corresponding hydrogen bonds in [2]pseudorotaxane **1b·2b**.[12] Along with the standard hydrogen bonds, the triptycene subunits also form multiple edge-to-face π···π stacking interactions in **3b** and C–H···π interactions in **4a** with the aromatic rings of squaraines. The key crystallographic distances show that both of the cavities of **1a** and **1b** became slightly larger after encapsulation of squaraine molecules than those of free macrocycles. Meanwhile, the shape of squaraine dyes also changed after being inserted into the cages, especially for **2e** in the *cis* [2]rotaxane **4a**, which became obviously curved and bent (Figure 2c and d). This phenomenon might result from the C–H···π interactions between the terminal benzyl stopper groups and the triptycene subunits. Relative to **2e** in [2]rotaxane **4a**, squaraine **2d** in [2]rotaxane **3b** kept its planar structure after threading the *trans* macrocycle **1b** (Figure 2a and b).

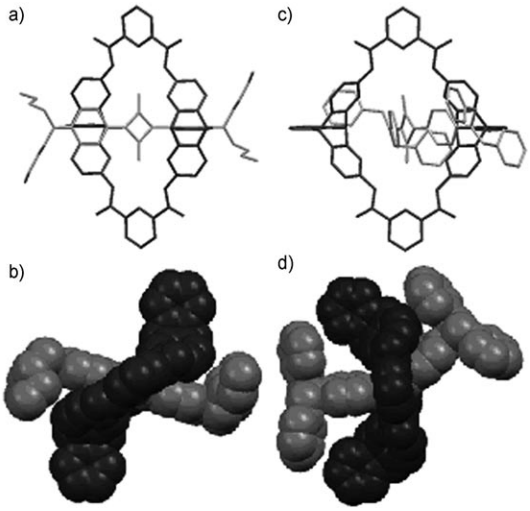

Figure 2. Crystal structures: a) Top view and b) side view of **3b**. c) Top view and d) side view of **4a**. Hydrogen atoms are omitted for clarity.

Optical properties of [2]rotaxanes: The absorption and emission properties of the [2]rotaxanes **3–5** and the relevant free squaraines were measured in $CHCl_3$. A direct comparison of [2]rotaxanes and the appropriate free squaraines revealed a redshift in both absorption (11–15 nm) and fluorescence emission (8–11 nm) (Table 2). The fluorescence quantum yields for the [2]rotaxanes were all decreased relative to those of free guests, but the *trans* isomeric [2]rotaxanes **3b**, **4b**, and **5c** showed higher quantum yields than those of *cis* isomers **3a**, **4a**, **5a**, and **5b**. We further investigated the chemical stabilities of these compounds by treating both the [2]rotaxanes and their corresponding squaraines with a large excess of L-cysteine in THF/H_2O 3:1 solutions. The subsequent time-dependent changes in absorption and emission for [2]rotaxanes **5** and squaraine **2g** are shown in Figure 3 and indicate that macrocycles **1a** and **1b** both provide steric shells for **2g** to prevent the attack by the nucleophilic species. It was also found that the *trans* isomers had better efficiency than the *cis* isomers, partially because of the location of the macrocycle **1b** on both sides of the cyclobutene core of squaraine derivatives. [2]Rotaxanes **4a** and **4b** showed relatively weak ability for protection of **2e**, possibly due to

Table 2. Photophysical properties for [2]rotaxanes **3–5** and the relevant free squaraines in $CHCl_3$.[a]

Compound	λ_{abs} [nm]	Log ε	λ_{em} [nm]	Φ_f [b]
2d	640	5.58	664	0.73
2e	630	5.53	654	0.70
2g	634	5.55	659	0.71
3a	653	5.46	673	0.49
3b	653	5.49	675	0.51
4a	643	5.45	665	0.27
4b	642	5.54	665	0.34
5a	649	5.49	670	0.47
5b	645	5.44	667	0.37
5c	647	5.49	669	0.55

[a] Solutions were excited at 580 nm and emission monitored in the region 590–750 nm for estimating Φ_f. [b] Fluorescence quantum yields were determined by using 4,4-[bis-(*N*,*N*-dimethylamino)phenyl] squaraine dye as the standard ($\Phi_f=0.7$ in $CHCl_3$); error limit ±5%.

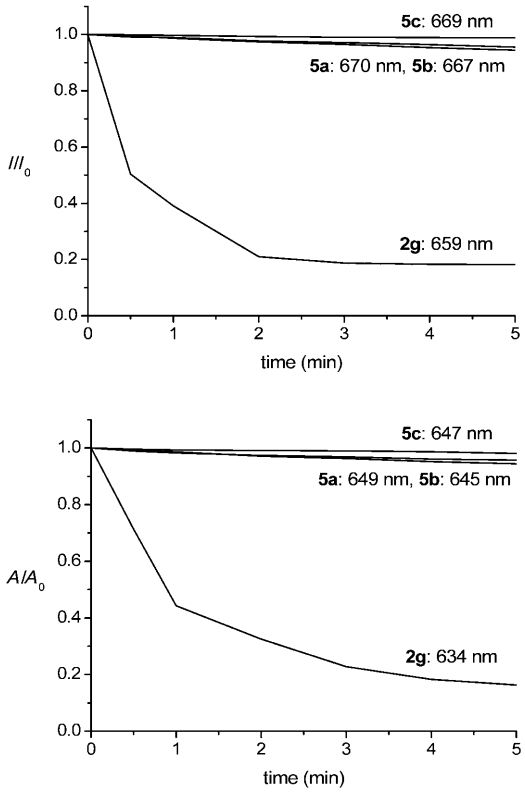

Figure 3. Changes in emission (top) and absorption (bottom) upon addition of L-cysteine (10 mM) to 1×10^{-5} M solutions of **2g** and **5a–c** in THF/H_2O 3:1 at 298 K.

the bulky stopper groups of squaraine that changed the shape of **2e** in the macrocycles (see the Supporting Information).

Tubular-assembled structures of [2]rotaxanes in the solid state: Interestingly, the structural studies on squaraine-based [2]rotaxanes **3b** and **4a** in the solid state revealed tubular assemblies consisting of molecules stacked above one another. In each case, the pore size of the porous column was defined by the cavity size of the wheel-like macrocycles, and squaraine molecules were encapsulated in the channels. Two intermolecular interactions dominated the assembly of **3b**, which were the offset π···π stacking interactions between squaraine **2d** of one [2]rotaxane molecule and the adjacent **2d** of another **3b** molecule with an interfacial distance of 3.44 Å (Figure 4a), and two C–H···π interactions ($d_{C-H\cdots\pi}$= 2.75, 2.76 Å) between the macrocycle **1b** of [2]rotaxane and toluene solvent molecules (Figure 4b). In the case of **4a**, the interactions that kept the [2]rotaxane molecules together included C–H···O hydrogen bonds ($d_{H\cdots O}$=2.43 Å, $\theta_{C-H\cdots O}$= 172.68°) and C–H···π interactions ($d_{C-H\cdots\pi}$=2.80, 2.84 Å) between squaraine **2e** of one [2]rotaxane molecule and macrocycle **1a** of another [2]rotaxane molecule (Figure 5a). Moreover, [2]rotaxane **4a** with nonsymmetrical macrocycles self-assembled together in an oriented arrangement (Figure 5b). Thus, an oriented nonsymmetrical channel-like structure was constructed in the solid state.[21] It was further found

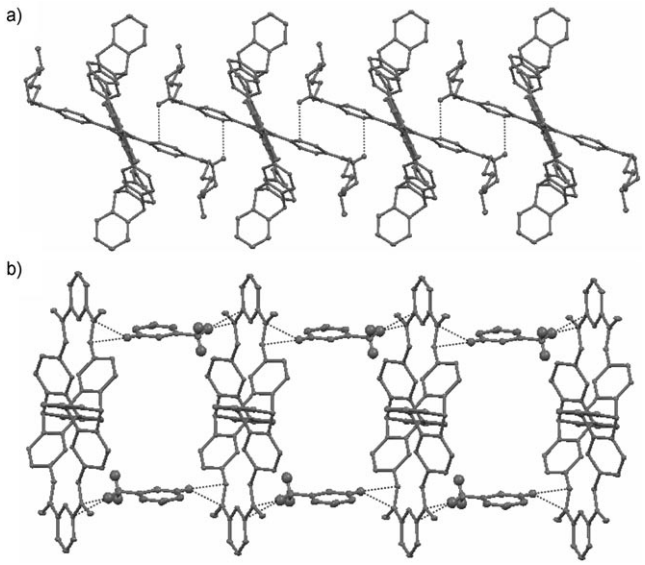

Figure 4. Packing of **3b**: Representation of the tubular structure and the noncovalent interactions (-----) between a) squaraines of different [2]rotaxane molecules (toluene molecules are omitted) and b) macrocycle host and toluene solvent (squaraine molecules are omitted). Hydrogen atoms not involved in the interactions are omitted for clarity.

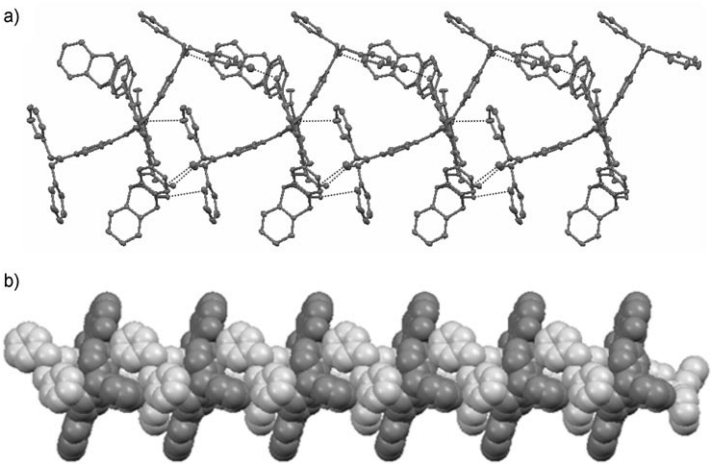

Figure 5. Packing of **4a**: Representation of a) the noncovalent interactions (-----) between macrocycle hosts and squaraines of different [2]rotaxane molecules and b) the oriented nonsymmetrical channel-like structure of **4a**. Hydrogen atoms not involved in the interactions are omitted for clarity.

that with the squaraine guests inside the macrocycles, in addition to the solvent interactions, macrocycles **1a** and **1b** in these [2]rotaxanes formed honeycombed suprastructures, which could not be seen in the free macrocycles (see the Supporting Information).

Conclusion

In summary, a series of [2]pseudorotaxanes and [2]rotaxanes based on the triptycene-derived macrocycles **1a–b** and

squaraines **2a–g** were constructed. As expected, we found that a new type of three-dimensional and nonsymmetrical macrocycle **1a** could form isomeric [2]rotaxanes due to the direction of the guest insertion with partial selection. Meanwhile, the different linking modes of triptycene derivatives also provided a new route to form isomeric [2]rotaxanes through the templated synthetic process. Consequently, in the case of [2]rotaxanes **5**, three isomers were simultaneously obtained from one reaction. Structural features and photophysical properties of these inclusion complexes were investigated, and it was found that the chemical stabilities of [2]rotaxanes **3–5** were increased relative to free squaraines. Moreover, we also found that the [2]rotaxanes **3b** and **4a** could self-assemble into a secondary arrangement of extended channels through multiple noncovalent interactions in the solid state, in which the squaraine molecules were inside as an axle. Especially for nonsymmetrical [2]rotaxane **4a**, an oriented channel-like suprastructure was formed. We believe that the method for construction of multiple isomeric [2]rotaxanes presented here can open unprecedented perspectives in the field of rotaxanes. Studies on the construction of unidirectional squaraine-based [2]rotaxanes based on this approach are underway in our laboratory.

Experimental Section

General: Melting points, taken on an electrothermal melting point apparatus, are uncorrected. The ^{1}H NMR and ^{13}C NMR spectra were measured on a Bruker DMX300 NMR spectrometer. 2D COSY and NOESY experiments were measured on a Bruker DMX600 NMR spectrometer. MALDI-TOF MS were obtained on a Bruker BIFLEXIII mass spectrometer. Elemental analyses were performed by the Analytical Laboratory of the Institute of Chemistry, CAS.

General procedure to synthesize squaraines 2a–e: The appropriate bisaniline derivatives (0.7 mmol) and triethyl orthoformate (2 mL) were added to a solution of squaric acid (0.35 mmol) in 2-propanol (50 mL) and the mixture was refluxed overnight. The reaction mixture was cooled and filtered and the pure product was obtained by washing the solid with methanol.

Procedure to synthesize squaraines 2f and 2g: Reaction of the appropriate dialkyl aniline derivatives and the squaryl chloride provided the semisquaraine intermediates according to the literature conditions.[15] The *N,N*-bisbenzylaniline (0.35 mmol), the appropriate semisquaraine intermediate (0.35 mmol), and triethyl orthoformate (2 mL) were added to a 100 mL flask containing 2-propanol (50 mL). The reaction mixture was then refluxed for 20 h. The hot reaction mixture was filtered and the solid was washed with 2-propanol. Column chromatography (chloroform/EtOAc 15:1) of the crude product over silica gel (100–200 mesh) gave the pure products **2f** and **2g**.

*Product **2f***: Yield: 34%; m.p. 223°C; ^{1}H NMR (300 MHz, $CDCl_3$): $\delta=$ 3.24 (s, 6H), 4.80 (s, 4H), 6.83 (d, $J=9$ Hz, 2H), 6.91 (d, $J=9$ Hz, 2H), 7.19–7.22 (m, 4H), 7.31–7.40 (m, 6H), 8.43 (d, $J=9$ Hz, 2H), 8.48 ppm (d, $J=9$ Hz, 2H); MALDI-TOF MS: m/z: 472.3 $[M]^+$; elemental analysis calcd (%) for $C_{32}H_{28}N_2O_2$: C 81.33, H 5.97, N 5.93; found: C 81.15, H 6.06, N 5.99.

*Product **2g***: Yield: 27%; m.p. 204°C; ^{1}H NMR (300 MHz, $CDCl_3$): $\delta=$ 0.98 (t, $J=7.3$ Hz, 6H), 1.33–1.46 (m, 4H), 1.59–1.69 (m, 4H), 3.44 (t, $J=$ 7.6 Hz, 4H), 4.78 (s, 4H), 6.71 (d, $J=9$ Hz, 2H), 6.86 (d, $J=9$ Hz, 2H), 7.20–7.22 (m, 4H), 7.26–7.38 (m, 6H), 8.34 (d, $J=9$ Hz, 2H), 8.38 ppm (d, $J=9$ Hz, 2H); ^{13}C NMR: (75 MHz, $CDCl_3$): $\delta=$13.9, 20.2, 29.6, 51.3, 54.0, 112.5, 112.9, 119.5, 120.9, 126.5, 127.7, 129.0, 132.8, 133.9, 136.2, 154.1, 154.3, 183.3, 187.2, 190.4 ppm; MALDI-TOF MS: m/z: 556.5 $[M]^+$; elemental analysis calcd (%) for $C_{38}H_{40}N_2O_2$: C 81.98, H 7.24, N 5.03; found: C 81.77, H 7.35, N 5.24.

General procedure to synthesize [2]rotaxanes 3–5: A solution of pyridine-2,6-dicarbonyl dichloride (0.2 mmol) in dry CH_2Cl_2 (10 mL) and a solution of 2,7-diaminotriptycene (0.2 mmol) in dry CH_2Cl_2 (10 mL) were added dropwise, respectively, into a solution of the relevant squaraine (0.1 mmol) and Et_3N (0.6 mmol) in dry CH_2Cl_2 (100 mL) at 0°C over a period of 2.5 h under an argon atmosphere. The mixture was stirred until it gradually warmed up to room temperature and was then stirred for 24 h. The solution was concentrated in vacuo and then the mixture was purified by column chromatography over silica gel (200–300 mesh) to afford the squaraine [2]rotaxanes **3–5**.

*Product **3a***: Yield: 17%; m.p. >300°C; ^{1}H NMR (300 MHz, $CDCl_3$): $\delta=$ 0.91 (t, $J=7.2$ Hz, 6H), 1.05 (t, $J=7.2$ Hz, 6H), 1.22–1.30 (m, 4H), 1.39–1.46 (m, 4H), 1.48–1.56 (m, 4H), 1.85–1.95 (m, 4H), 3.19 (t, $J=7.2$ Hz, 4H), 3.71 (t, $J=7.5$ Hz, 4H), 4.46 (s, 2H), 5.26 (s, 2H), 6.13 (d, $J=9$ Hz, 2H), 6.86–6.91 (m, 4H), 6.96–7.01 (m, 2H), 7.20 (d, $J=8$ Hz, 4H), 7.33–7.35 (m, 4H), 7.39 (d, $J=1$ Hz, 4H), 7.45 (d, $J=9.0$ Hz, 2H), 7.69 (dd, $J=8$, 1 Hz, 4H), 8.12 (t, $J=7.8$ Hz, 2H), 8.54 (d, $J=7.8$ Hz, 4H), 9.26 (d, $J=9$ Hz, 2H), 11.19 ppm (s, 4H); ^{13}C NMR (75 MHz, $CDCl_3$): $\delta=$13.8, 13.9, 20.1, 20.4, 29.5, 29.7, 51.4, 51.7, 52.8, 53.1, 112.7, 113.8, 117.9, 118.9, 123.28, 123.32, 123.5, 124.8, 125.3, 125.4, 132.7, 133.3, 134.5, 138.8, 141.6, 144.0, 144.7, 145.7, 149.8, 153.1, 162.1, 185.6 ppm; MALDI TOF-MS: m/z: 1318.9 $[M]^+$; elemental analysis calcd (%) for $C_{86}H_{78}N_8O_6{\cdot}0.5\,H_2O$: C 77.75, H 5.99, N 8.43; found: C 77.57, H 6.13, N 8.20.

*Product **3b***: Yield: 15%; m.p. >300°C; ^{1}H NMR (300 MHz, $CDCl_3$): $\delta=$ 1.10 (t, $J=6.3$ Hz, 12H), 1.43–1.48 (m, 8H), 1.63–1.74 (m, 8H), 3.41 (br, 8H), 4.85 (s, 2H), 5.10 (s, 2H), 6.39 (d, $J=6.2$ Hz, 4H), 6.80–6.93 (m, 8H), 7.06–7.11 (m, 6H), 7.23–7.25 (m, 2H), 7.55 (d, $J=7.3$ Hz, 4H), 7.64 (d, $J=6.2$ Hz, 4H), 8.12 (t, $J=7.7$ Hz, 2H), 8.50 (d, $J=7.7$ Hz, 4H), 11.26 ppm (s, 4H); ^{13}C NMR (75 MHz, $CDCl_3$): $\delta=$14.1, 20.3, 29.6, 52.10, 52.13, 52.71, 53.71, 113.4, 118.2, 119.2, 119.9, 122.8, 123.3, 123.5, 125.0, 125.3, 132.3, 134.2, 139.1, 141.7, 144.1, 144.5, 145.3, 149.4, 162.0, 185.3 ppm; MALDI TOF-MS: m/z: 1318.9 $[M]^+$, 1341.9 $[M+Na]^+$, 1358.0 $[M+K]^+$; elemental analysis calcd (%) for $C_{86}H_{78}N_8O_6$: C 78.28, H 5.96, N 8.49; found: C 78.07, H 6.13, N 8.32.

*Product **4a***: Yield: 18%; m.p. 282–283°C; ^{1}H NMR (600 MHz, $CDCl_3$): $\delta=$4.45 (s, 2H), 4.54 (s, 4H), 5.08 (s, 4H), 5.26 (s, 2H), 6.23 (d, $J=9$ Hz, 2H), 6.96–7.00 (m, 8H), 7.03 (t, $J=7.1$ Hz, 2H), 7.16 (d, $J=8$ Hz, 4H), 7.29 (d, $J=1$ Hz, 4H), 7.30–7.35 (m, 8H), 7.37 (d, $J=7.3$ Hz, 2H), 7.40–7.43 (m, 10H), 7.46 (d, $J=9$ Hz, 2H), 7.58 (dd, $J=8$, 1 Hz, 4H), 8.06 (t, $J=7.7$ Hz, 2H), 8.47 (d, $J=7.7$ Hz, 4H), 9.24 (d, $J=8.8$ Hz, 2H), 11.07 ppm (s, 4H); ^{13}C NMR (75 MHz, $CDCl_3$): $\delta=$52.8, 53.3, 53.9, 54.7, 112.9, 114.6, 117.9, 119.1, 119.2, 120.3, 123.3, 123.6, 124.9, 125.3, 125.5, 126.2, 126.4, 128.0, 128.20, 128.24, 129.05, 129.13, 129.4, 132.9, 133.8, 134.3, 135.1, 135.7, 138.8, 141.6, 143.9, 144.7, 145.6, 149.6, 154.9, 155.7, 162.0, 181.1, 185.2, 187.2 ppm; MALDI TOF-MS: m/z: 1454.8 $[M]^+$, 1477.9 $[M+Na]^+$, 1493.9 $[M+K]^+$; elemental analysis calcd (%) for $C_{98}H_{70}N_8O_6{\cdot}H_2O$: C 79.87, H 4.92, N 7.60; found: C 79.82, H 4.93, N 7.70.

*Product **4b***: Yield: 14%; m.p. >300°C; ^{1}H NMR (300 MHz, [D$_6$]DMSO): $\delta=$4.94 (s, 10H), 5.22 (s, 2H), 6.23 (d, $J=9.2$ Hz, 2H), 6.96–7.00 (m, 8H), 7.03 (t, $J=7.1$ Hz, 2H), 7.16 (d, $J=8$ Hz, 4H), 7.29 (d, $J=1$ Hz, 4H), 7.30–7.35 (m, 8H), 7.37 (d, $J=7.3$ Hz, 2H), 7.40–7.43 (m, 10H), 7.46 (d, $J=8.8$ Hz, 2H), 7.58 (dd, $J=8$, 1 Hz, 4H), 8.06 (t, $J=$ 7.7 Hz, 2H), 8.47 (d, $J=7.7$ Hz, 4H), 9.24 (d, $J=8.8$ Hz, 2H), 11.07 ppm (s, 4H); MALDI TOF-MS: m/z: 1454.8 $[M]^+$, 1477.9 $[M+Na]^+$; elemental analysis calcd (%) for $C_{98}H_{70}N_8O_6{\cdot}0.8\,H_2O$: C 80.07, H 4.91, N 7.62; found: C 80.02, H 5.13, N 7.54.

*Product **5a***: Yield: 16%; m.p. >292°C; ^{1}H NMR (600 MHz, $CDCl_3$): $\delta=$ 1.05 (t, $J=7.3$ Hz, 6H), 1.49–1.55 (m, 4H), 1.87–1.92 (m, 4H), 3.72 (t, $J=$ 7.8 Hz, 4H), 4.45 (s, 2H), 4.53 (s, 4H), 5.25 (s, 2H), 6.21 (d, $J=9.3$ Hz, 2H), 6.87–6.92 (m, 4H), 6.97–7.00 (m, 6H), 7.15 (d, $J=8$ Hz, 4H), 7.31 (d, $J=9$ Hz, 2H), 7.31–7.36 (m, 12H), 7.37 (d, $J=9.3$ Hz, 2H), 7.57 (dd, $J=8$, 2 Hz, 4H), 8.07 (t, $J=7.7$ Hz, 2H), 8.49 (d, $J=7.7$ Hz, 4H), 9.25 (d, $J=9$ Hz, 2H), 11.11 ppm (s, 4H); ^{13}C NMR (75 MHz, $CDCl_3$): $\delta=$13.9, 20.4, 29.71, 29.74, 51.7, 52.8, 53.1, 53.8, 112.6, 113.9, 118.0, 119.1, 119.3, 123.3, 123.6, 124.7, 125.3, 125.4, 126.2, 127.9, 129.1, 133.1, 133.5, 134.3,

135.4, 138.8, 141.6, 143.9, 144.7, 145.6, 149.6, 153.9, 154.9, 162.0, 182.0, 185.3, 185.4 ppm; MALDI TOF-MS: *m/z*: 1386.9 $[M]^+$, 1409.9 $[M+Na]^+$, 1426.0 $[M+K]^+$; elemental analysis calcd (%) for $C_{92}H_{74}N_8O_6 \cdot H_2O$: C 78.61, H 5.45, N 7.97; found: C 78.56, H 5.33, N 7.77.

Product ***5b***: Yield: 9%; m.p. >300°C; ^{1}H NMR (600 MHz, $CDCl_3$): $\delta =$ 0.96 (t, $J=7.4$ Hz, 6H), 1.41–1.47 (m, 4H), 1.70–1.74 (m, 4H), 3.20 (t, $J=$ 7.8 Hz, 4H), 4.47 (s, 2H), 5.08 (s, 4H), 5.27 (s, 2H), 6.09 (d, $J=9$ Hz, 2H), 6.97–7.00 (m, 4H), 7.20 (d, $J=8.0$ Hz, 4H), 7.36–7.37 (m, 4H), 7.40–7.42 (m, 6H), 7.45 (d, $J=9$ Hz, 2H), 7.48 (d, $J=9$ Hz, 2H), 7.52–7.53 (m, 4H), 7.69 (dd, $J=8.0$, 1.8 Hz, 4H), 7.71–7.72 (m, 4H), 8.10 (t, $J=7.7$ Hz, 2H), 8.51 (d, $J=7.7$ Hz, 4H), 9.23 (d, $J=9$ Hz, 2H), 11.16 ppm (s, 4H); ^{13}C NMR (75 MHz, $CDCl_3$): $\delta =$13.0, 21.6, 28.2, 50.3, 51.7, 53.5, 55.7, 113.2, 116.6, 117.7, 122.2, 123.74, 123.77, 124.1, 124.4, 125.3, 126.9, 127.7, 128.2, 129.8, 131.2, 132.76, 132.80, 133.0, 133.3, 134.1, 134.9, 137.7, 140.4, 142.8, 143.6, 144.6, 148.6, 160.9, 166.6, 183.1, 184.4 ppm; MALDI TOF-MS: *m/z*: 1386.8 $[M]^+$, 1409.8 $[M+Na]^+$, 1425.8 $[M+K]^+$; elemental analysis calcd (%) for $C_{92}H_{74}N_8O_6 \cdot 1.5\,H_2O$: C 78.11, H 5.49, N 7.92; found: C 77.97, H 5.28, N 7.88.

Product ***5c***: Yield: 12%; m.p. >300°C; ^{1}H NMR (600 MHz, $CDCl_3$): $\delta =$ 1.09 (t, $J=7.4$ Hz, 6H), 1.44–1.50 (m, 4H), 1.65–1.70 (m, 4H), 3.40 (t, $J=$ 7.6 Hz, 4H), 4.77 (s, 4H), 4.83 (s, 1H), 4.87 (s, 1H), 5.10 (s, 2H), 6.22 (d, $J=9$ Hz, 2H), 6.37 (d, $J=9$ Hz, 2H), 6.82–6.86 (m, 4H), 6.87 (d, $J=2$ Hz, 2H), 6.89 (d, $J=8$ Hz, 2H), 6.91 (d, $J=8.0$ Hz, 2H), 7.06 (d, $J=7.3$ Hz, 2H), 7.08 (d, $J=8$ Hz, 2H), 7.24–7.26 (m, 4H), 7.30 (d, $J=7.4$ Hz, 2H), 7.40–7.44 (m, 4H), 7.46 (dd, $J=8$, 2 Hz, 2H), 7.51–7.54 (m, 6H), 7.62 (dd, $J=8$, 2 Hz, 2H), 8.10 (t, $J=7.7$ Hz, 2H), 8.46 (d, $J=7.7$ Hz, 2H), 8.47 (d, $J=7.7$ Hz, 2H), 11.23 (s, 2H), 11.24 ppm (s, 2H); ^{13}C NMR (75 MHz, $CDCl_3$): $\delta =$14.1, 20.3, 30.0, 51.5, 52.1, 52.8, 53.7, 54.5, 112.4, 112.5, 119.18, 119.23, 119.78, 119.81, 120.1, 122.7, 123.0, 123.2, 123.3, 123.4, 124.9, 125.3, 126.4, 126.5, 127.98, 128.01, 129.2, 132.0, 132.9, 134.0, 134.2, 136.5, 139.1, 141.6, 141.7, 144.1, 145.2, 145.3, 149.5, 153.3, 161.9, 162.0, 185.2 ppm; MALDI TOF-MS: *m/z*: 1386.8 $[M]^+$, 1409.9 $[M+Na]^+$, 1425.9 $[M+K]^+$; elemental analysis calcd (%) for $C_{92}H_{74}N_8O_6 \cdot H_2O$: C 78.61, H 5.45, N 7.97; found: C 78.42, H 5.19, N 8.11.

Acknowledgements

We thank the National Natural Science Foundation of China (20625206, 20972162), the Chinese Academy of Sciences, and the National Basic Research Program (2007CB808004, 2009ZX09501-018) for financial support.

[1] a) V. Balzani, A. Credi, M. Venturi, *Molecular Devices and Machines—Concepts and Perspectives for the Nanoworld*, 2nd ed., Wiley-VCH, Weinheim, **2008**; b) B. L. Feringa, *Molecular Switches*, Wiley-VCH, Weinheim, **2001**.

[2] a) H. Tian, Q. C. Wang, *Chem. Soc. Rev.* **2006**, *35*, 361–374; b) E. R. Kay, D. A. Leigh, F. Zerbetto, *Angew. Chem.* **2007**, *119*, 72–196; *Angew. Chem. Int. Ed.* **2007**, *46*, 72–191; c) C. A. Schalley, T. Weilandt, J. Bruggemann, F. Vögtle, *Top. Curr. Chem.* **2005**, *248*, 141–200.

[3] a) R. Isnin, A. E. Kaifer, *J. Am. Chem. Soc.* **1991**, *113*, 8188–8190; b) R. Isnin, A. Kaifer, *Pure Appl. Chem.* **1993**, *65*, 495–498.

[4] a) Q.-C. Wang, X. Ma, D.-H. Qu, H. Tian, *Chem. Eur. J.* **2006**, *12*, 1088–1096; b) X. Ma, Q.-C. Wang, H. Tian, *Tetrahedron Lett.* **2007**, *48*, 7112–7116.

[5] a) A. Arduini, F. Calzavacca, A. Pochini, A. Secchi, *Chem. Eur. J.* **2003**, *9*, 793–799; b) A. Credi, S. Dumas, S. Silvi, M. Venturi, A. Arduini, A. Pochini, A. Secchi, *J. Org. Chem.* **2004**, *69*, 5881–5887; c) A. Arduini, F. Ciesa, M. Fragassi, A. Pochini, A. Secchi, *Angew. Chem.* **2005**, *117*, 282–285; *Angew. Chem. Int. Ed.* **2005**, *44*, 278–281; d) A. Arduini, R. Bussolati, A. Credi, A. Pochini, A. Secchi, S. Silvi, M. Venturi, *Tetrahedron* **2008**, *64*, 8279–8286; e) A. Arduini, R. Bussolati, A. Credi, G. Faimani, S. Garaudée, A. Pochini, A. Secchi, M. Semeraro, S. Silvi, M. Venturi, *Chem. Eur. J.* **2009**, *15*, 3230–3242.

[6] a) S. Sreejith, P. Carol, P. Chithraa, A. Ajayaghosh, *J. Mater. Chem.* **2008**, *18*, 264–274; b) J. J. Mcewen, K. J. Wallace, *Chem. Commun.* **2009**, 6339–6351.

[7] a) H. Chen, M. S. Farahat, K. Y. Law, D. G. Whitten, *J. Am. Chem. Soc.* **1996**, *118*, 2584–2594; b) J. V. Ros-Lis, B. García, D. Jiménez, R. Martínez-Máñez, F. Sancenón, J. Soto, F. Gonzalvo, M. C. Valldecabres, *J. Am. Chem. Soc.* **2004**, *126*, 4064–4065.

[8] a) E. Arunkumar, C. C. Forbes, B. C. Noll, B. D. Smith, *J. Am. Chem. Soc.* **2005**, *127*, 3288–3289; b) J. J. Gassensmith, J. M. Baumes, B. D. Smith, *Chem. Commun.* **2009**, 6329–6338, and references therein; c) S. Xiao, N. Fu, K. Packham, B. D. Smith, *Org. Lett.* **2010**, *12*, 140–143; d) J.-J. Lee, A. G. White, J. M. Baumes, B. D. Smith, *Chem. Commun.* **2010**, *46*, 1068–1069.

[9] a) J. R. Johnson, N. Fu, E. Arunkumar, W. M. Leevy, S. T. Gammon, D. Piwnica-Worms, B. D. Smith, *Angew. Chem.* **2007**, *119*, 5624–5627; *Angew. Chem. Int. Ed.* **2007**, *46*, 5528–5531; b) J. J. Gassensmith, S. Matthys, J.-J. Lee, A. Wojcik, P. V. Kamat, B. D. Smith, *Chem. Eur. J.* **2010**, *16*, 2916–2921.

[10] a) S.-Y. Hsueh, C.-C. Lai, Y.-H. Liu, S.-M. Peng, S.-H. Chiu, *Angew. Chem.* **2007**, *119*, 2059–2063; *Angew. Chem. Int. Ed.* **2007**, *46*, 2013–2017; b) S. Y. Hsueh, C. C. Lai, Y. H. Liu, S. M. Peng, S. H. Chiu, *Org. Lett.* **2007**, *9*, 4523–4526.

[11] a) X.-Z. Zhu, C.-F. Chen, *J. Am. Chem. Soc.* **2005**, *127*, 13158–13159; b) Q.-S. Zong, C.-F. Chen, *Org. Lett.* **2006**, *8*, 211–214; c) T. Han, C.-F. Chen, *Org. Lett.* **2006**, *8*, 1069–1072; d) X.-X. Peng, H.-Y. Lu, T. Han, C.-F. Chen, *Org. Lett.* **2007**, *9*, 895–898; e) X.-Z. Zhu, C.-F. Chen, *Chem. Eur. J.* **2006**, *12*, 5603–5609; f) C. Zhang, C.-F. Chen, *J. Org. Chem.* **2006**, *71*, 6626–6629; g) J.-M. Zhao, Q.-S. Zong, T. Han, J.-F. Xiang, C.-F. Chen, *J. Org. Chem.* **2008**, *73*, 6800–6806.

[12] M. Xue, C.-F. Chen, *Chem. Commun.* **2008**, 6128–6130.

[13] Examples for isomeric macrocycles as diastereomers based on different linking modes of triptycene derivatives: a) C. Zhang, C.-F. Chen, *J. Org. Chem.* **2007**, *72*, 3880–3888; b) M. Xue, C.-F. Chen, *Org. Lett.* **2009**, *11*, 5294–5297; c) X.-H. Tian, X. Hao, T.-L. Liang, C.-F. Chen, *Chem. Commun.* **2009**, 6771–6773; d) X.-H. Tian, C.-F. Chen, *Org. Lett.* **2010**, *12*, 524–527.

[14] G. J. Ashwell, G. S. Bahra, C. R. Brown, D. G. Hamilton, C. H. L. Kennard, D. E. Lynch, *J. Mater. Chem.* **1996**, *6*, 23–26.

[15] E. Arunkumar, P. Chithra, A. Ajayaghosh, *J. Am. Chem. Soc.* **2004**, *126*, 6590–6598.

[16] In this case, signals of macrocycle **1a** displayed little shift, possibly due to the weak interactions between the macrocyclic host and the adjacent squaraine molecule **2c** outside the macrocycle.

[17] The yield of each isomer for [2]rotaxanes **3**–**5** is shown in Scheme 4.

[18] The nonsymmetrical environment induced by macrocycle **1a** also appeared in complex **1a·2b** as judged by the ^{1}H NMR spectrum (see reference [12]).

[19] See the Figure S24 in the Supporting Information.

[20] CCDC-770092 (**3b**) and 770093 (**4a**) contain the supplementary crystallographic data for this paper. These data can be obtained free of charge from The Cambridge Crystallographic Data Centre via www.ccdc.cam.ac.uk/data_request/cif.

[21] An example for an oriented channel-like structure: A. Arduini, A. Credi, G. Faimani, C. Massera, A. Pochini, A. Secchi, M. Semeraro, S. Silvi, F. Ugozzoli, *Chem. Eur. J.* **2008**, *14*, 98–106.

Received: March 27, 2010
Published online: June 10, 2010

